

Supplementary Information accompanying

An epigenetic mechanism of resistance to targeted therapy in T-cell acute lymphoblastic leukemia

Birgit Knoechel^{1,2,3,4*}, Justine E. Roderick^{5*}, Kaylyn E. Williamson^{1,2,6,7}, Jiang Zhu^{1,2,6,7}, Jens G. Lohr^{2,8}, Matthew J. Cotton^{1,2,6,7}, Shawn M. Gillespie^{1,2,6,7}, Daniel Fernandez^{2,9}, Manching Ku^{1,2,6}, Hongfang Wang¹⁰, Federica Piccioni², Serena J. Silver², Mohit Jain^{2,11}, Daniel Pearson^{4,12}, Michael J. Kluk¹⁰, Christopher J. Ott⁸, Leonard D. Shultz¹³, Michael A. Brehm¹⁴, Dale L. Greiner¹⁴, Alejandro Gutierrez^{3,4}, Kimberly Stegmaier^{3,4}, Andrew L. Kung^{3,4}, David E. Root², James E. Bradner^{2,8}, Jon C. Aster¹⁰, Michelle A. Kelliher⁵, Bradley E. Bernstein^{1,2,6,7}

¹ Department of Pathology, Massachusetts General Hospital and Harvard Medical School, Boston, MA 02114, USA

² Broad Institute of MIT and Harvard, Cambridge, MA 02142, USA

³ Department of Pediatric Oncology, Dana-Farber Cancer Institute, Boston, MA 02215, USA

⁴ Division of Hematology/Oncology, Boston Children's Hospital and Harvard Medical School, Boston, MA 02115, USA

⁵ Department of Cancer Biology, University of Massachusetts Medical School, 364 Plantation Street, Worcester, MA 01605, USA

⁶ Center for Cancer Research, Massachusetts General Hospital, Boston, MA 02114, USA

⁷ Howard Hughes Medical Institute, Chevy Chase, MD 20815, USA

⁸ Department of Medical Oncology, Dana-Farber Cancer Institute, Boston, MA 02215, USA

⁹ Biostatistics Graduate Program, Harvard University, Cambridge, MA 02138, USA

¹⁰ Department of Pathology, Brigham and Women's Hospital and Harvard Medical School, Boston, MA 02115, USA

¹¹ Center for Human Genetic Research and Department of Molecular Biology, Massachusetts General Hospital, Boston, MA 02114, USA

¹² Biological and Biomedical Sciences Graduate Program, Harvard Medical School, Boston, MA 02215, USA

¹³ The Jackson Laboratory, Bar Harbor, ME 04609, USA

¹⁴ Program in Molecular Medicine, University of Massachusetts Medical School, Worcester, MA 01655, USA

Address correspondence to Bernstein.Bradley@mgh.harvard.edu and Michelle.Kelliher@umassmed.edu

* Equal contributions

Inventory of Supplementary Information

Supplementary Figures

Supplementary Figure 1

Supplementary Figure 2

Supplementary Figure 3

Supplementary Figure 4

Supplementary Figure 5

Supplementary Figure 6

Supplementary Figure 7

Supplementary Tables

Supplementary Table 1

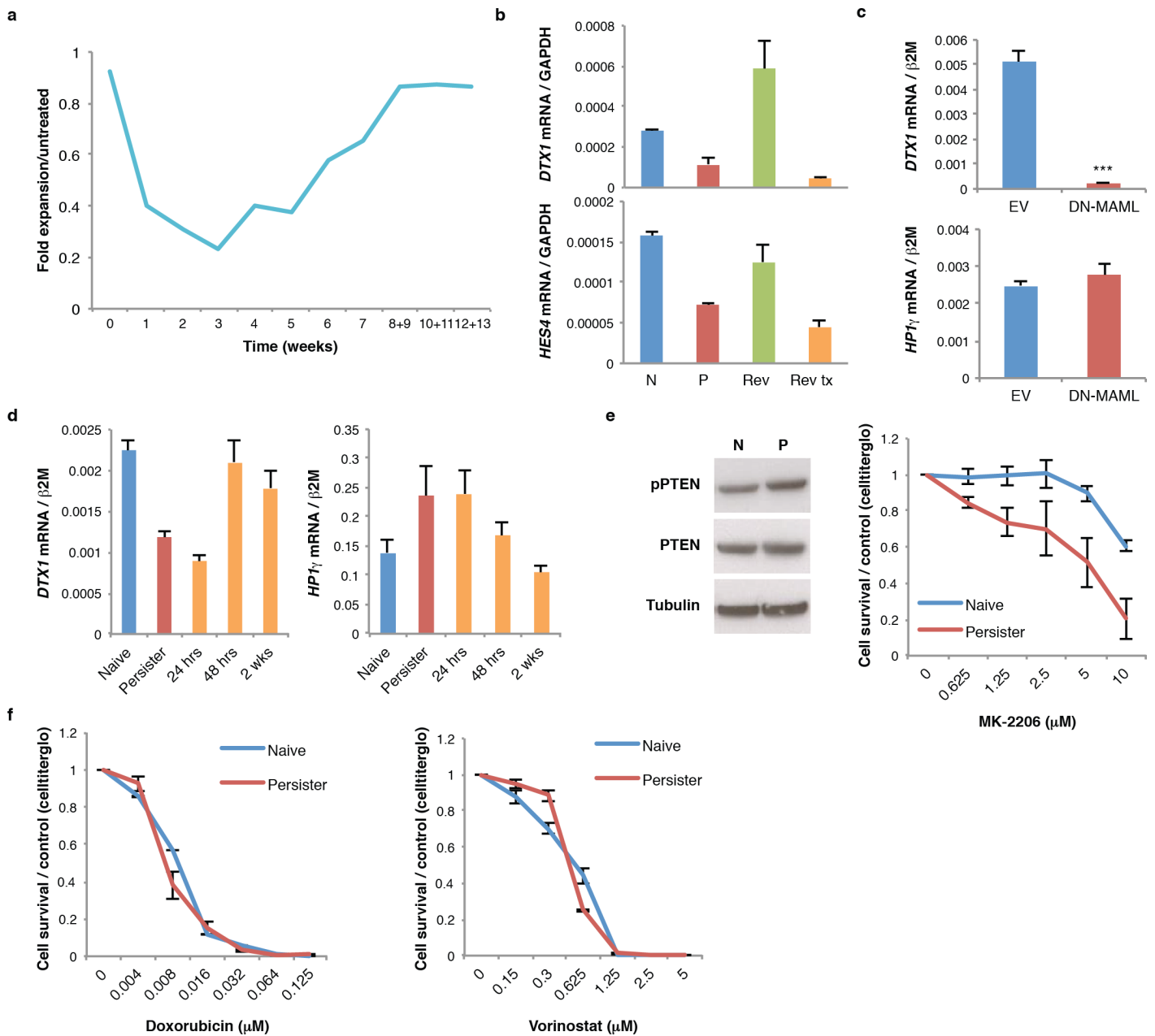
Supplementary Table 2

Supplementary Table 3

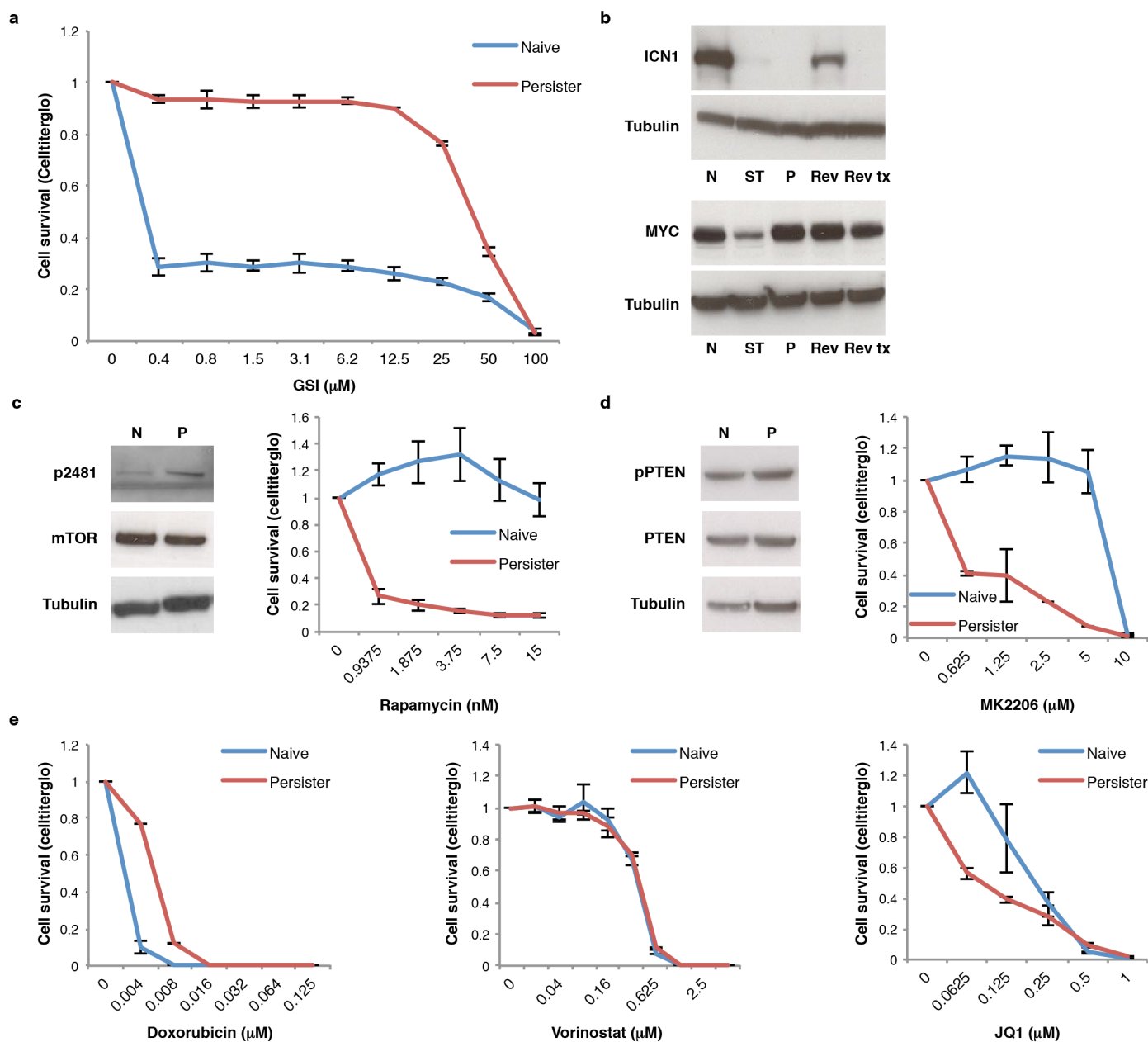
Supplementary Table 4

Supplementary Table 5

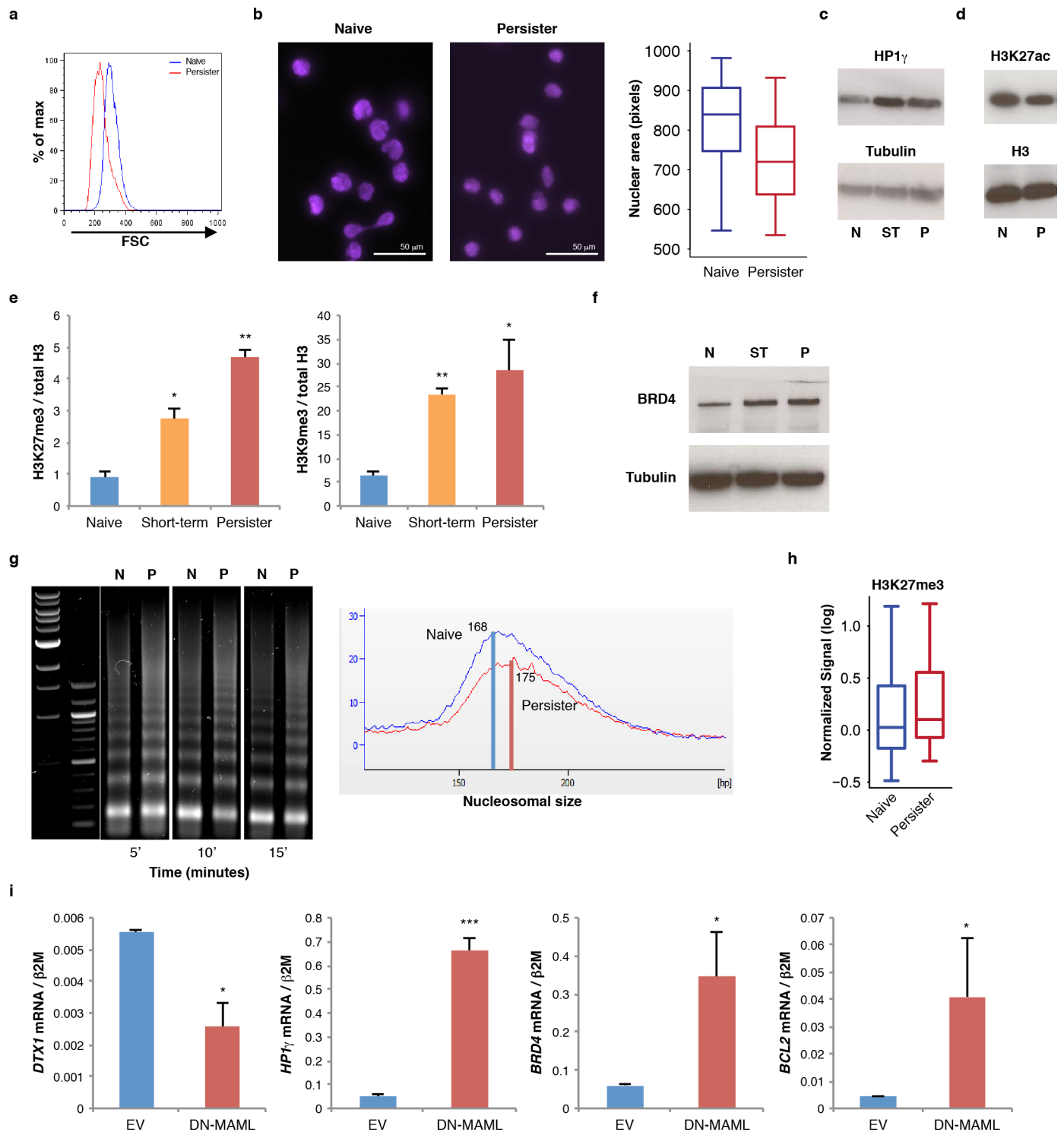
Supplementary Note



Supplementary Figure 1. Isolation and characterization of persister T-ALL cells. **a.** Proliferation over time is shown for naïve DND-41 T-ALL cells exposed to 1 μ M GSI. **b.** NOTCH1 target gene expression is shown for naïve cells (N), persister cells in 1 μ M GSI (P), ‘reversed’ persister cells removed from GSI for 2 weeks (Rev) and reversed cells re-exposed to 1 μ M GSI for 5 days (Rev tx) (2 replicates, error bars reflect s.d.). **c.** *DTX1* and *HP1 γ* gene expression is shown for naïve cells 4 weeks after transfection with dominant-negative mastermind-like 1 (DN-MAML) (3 replicates, error bars reflect s.d.). **d.** *DTX1* and *HP1 γ* gene expression is shown for naïve and persister cells, and for persister cells after GSI washout at the indicated time points (3 replicates, error bars reflect s.d.). **e.** Western blots for total, phosphorylated PTEN (pPTEN) and Tubulin in naïve and persister cells (left). Persister cells show decreased PTEN activity. Proliferation of naïve and persister cells treated with the indicated doses of the AKT inhibitor MK-2206 for 6 days (right; 4 replicates, error bars reflect s.d.). **f.** Proliferation of naïve and persister cells treated with the indicated doses of Doxorubicin (2 replicates, error bars reflect s.d.) and Vorinostat (2 replicates, error bars reflect s.d.) for 6 days. (Data shown for DND-41 cells.)

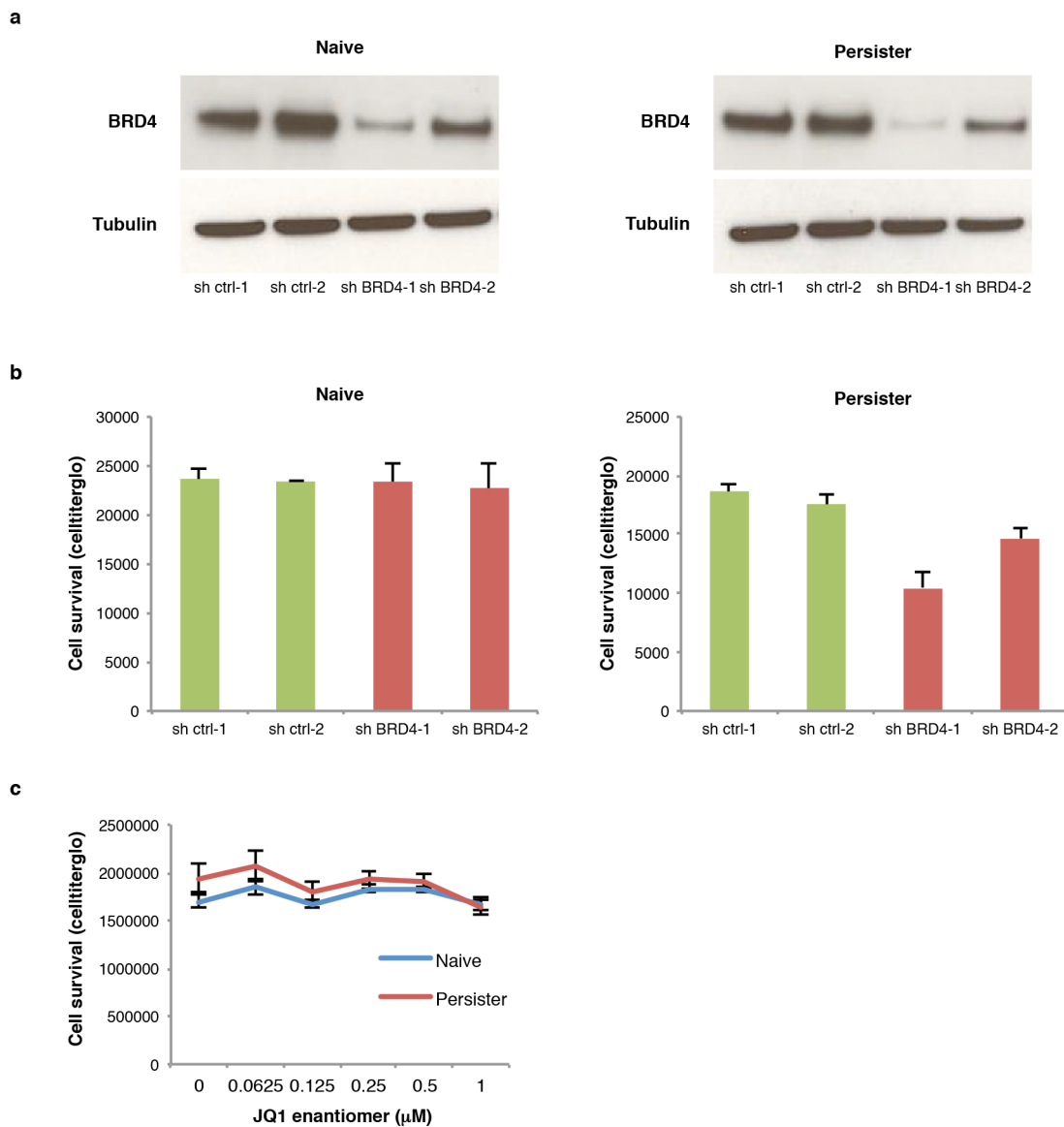


Supplementary Figure 2. Altered signaling and drug sensitivities in KOPT-K1 persister cells. **a.** Proliferation of naïve and persister KOPT-K1 T-ALL cells treated with the indicated doses of NOTCH inhibitor for 6 days (2 replicates, error bars reflect s.d.). **b.** Western blot shows activated intracellular NOTCH1 (ICN1) and MYC levels in naïve KOPT-K1 cells (N), short-term treated cells (ST, 5 days with 1 μM GSI), persister cells in 1 μM GSI (P), ‘reversed’ persister cells removed from GSI for 1 week (Rev), and reversed cells re-exposed to GSI (Rev tx, 5 days). **c.** Western blots show phospho-mTOR (p2481), total mTOR and Tubulin in naïve (N), and persister (P) KOPT-K1 cells (left). Proliferation of naïve and persister cells treated with indicated concentrations of Rapamycin for 9 days is shown at right (2 replicates, error bars reflect s.d.). **d.** Western blots for total, phosphorylated PTEN (pPTEN) and Tubulin in naïve and persister KOPT-K1 cells (left). Proliferation of naïve and persister cells treated with the indicated doses of the AKT inhibitor MK-2206 for 9 days (right; 2 replicates, error bars reflect s.d.). **e.** Proliferation of naïve and persister cells treated with the indicated doses of Doxorubicin, Vorinostat and JQ1 for 6 days (2 – 3 replicates, error bars reflect s.d.). These data confirm that KOPT-K1 cells give rise to a persister phenotype similar to DND-41 cells (see Figure 1).

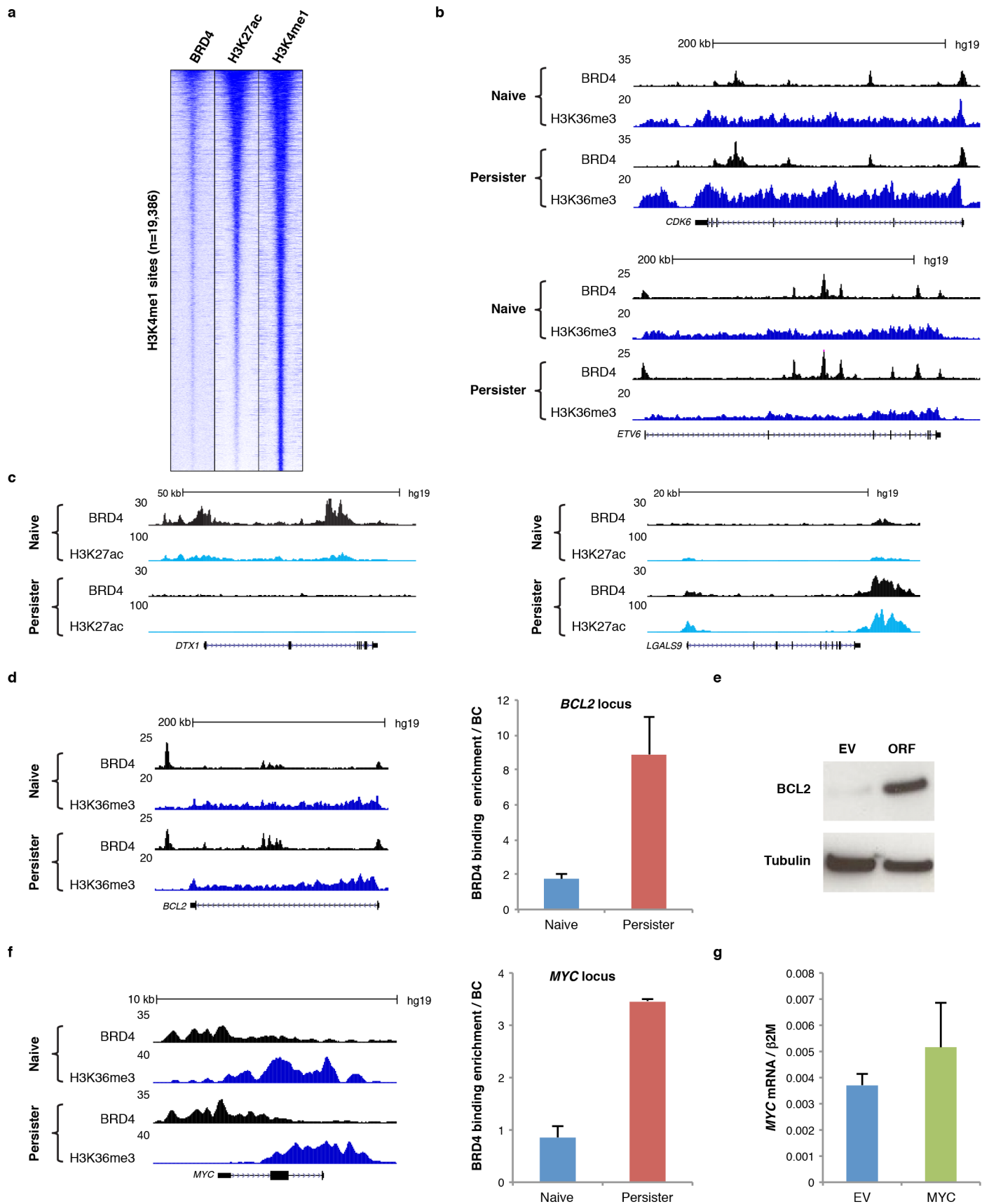


Supplementary Figure 3. Chromatin state alterations in KOPT-K1 persister cells. **a.** Forward scatter analysis indicates size distributions of naïve (blue) and persister (red) KOPT-K1 T-ALL cells. **b.** Size of naïve (left) and persister (right) KOPT-K1 cell nuclei is shown by DAPI stain and quantified in box plot (right; naïve $n = 316$, persister $n = 396$; p value $< 10^{-4}$). **c, d.** Western blots for HP1 γ (c) and H3K27ac and total H3 (d) in naïve (N) and persister (P) KOPT-K1 cells. **e.** Bar plot indicates relative levels of repressive histone modifications per ELISA of bulk histones from naïve, short-term treated (3 days) and persister cells (2 replicates, error bars reflect s.d., * = p value < 0.05 , ** = p value < 0.01). **f.** BRD4 expression is shown for naïve (N), short-term treated (ST, 5 days) and persister (P) KOPT-K1 cells. These data show that persister KOPT-K1 cells exhibit chromatin

state changes similar to DND-41 cells (see Figure 2). **g.** Gel electrophoresis images depict size distribution of DNA after MNase digestion of chromatin from naïve (N) or persister (P) KOPT-K1 cells (left). Plot depicts size distribution of mononucleosomal DNA fragments after MNase digestion, as measured by capillary electrophoresis (right). Protected regions are larger in persister compared to naïve cells, consistent with greater chromatin compaction. **h.** Normalized H3K27me3 signal distribution over euchromatic H3K4me1-marked loci in naïve and persister KOPT-K1 cells (p value < 10^{-15}). **i.** *DTX1*, *HP1 γ* , *BRD4* and *BCL2* expression are shown for KOPT-K1 cells 4 weeks post-transfection with DN-MAML or empty vector (EV), (2 replicates, error bars reflect s.d., * = p value < 0.05, *** = p value < 0.001). These data confirm that KOPT-K1 persister cells adopt an altered chromatin state similar to DND-41 persister cells (see Figure 2).

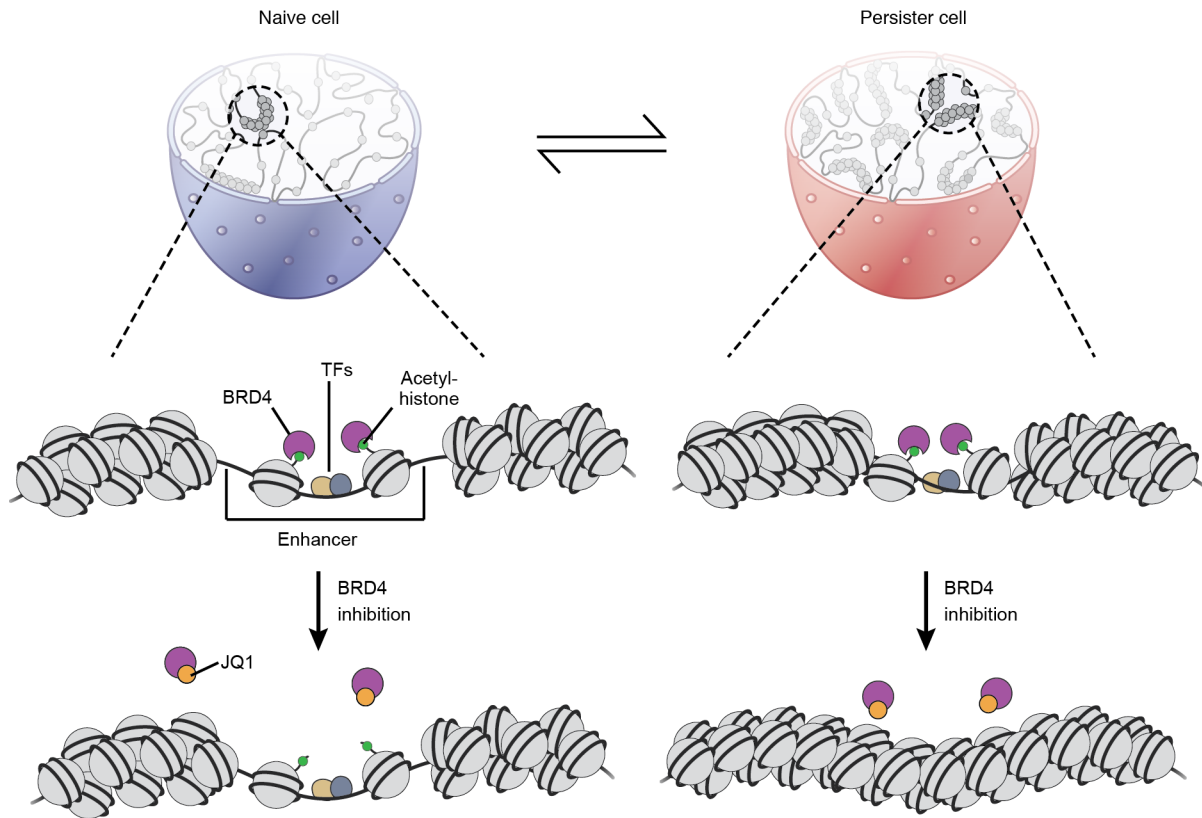


Supplementary Figure 4. Persister T-ALL cells have increased dependency on BRD4. **a.** Western blots show BRD4 expression after knockdown with lentiviral shRNA in naïve and persister DND-41 cells after 5 days of puromycin selection (2 replicates, error bars reflect s.d.). **b.** Proliferative response of naïve and persister cells infected with BRD4 or control hairpins after 8 days of puromycin selection. **c.** Proliferative response of naïve and persister cells after 6 days treatment with inactive JQ1 enantiomer (3 replicates, error bars reflect s.d.).

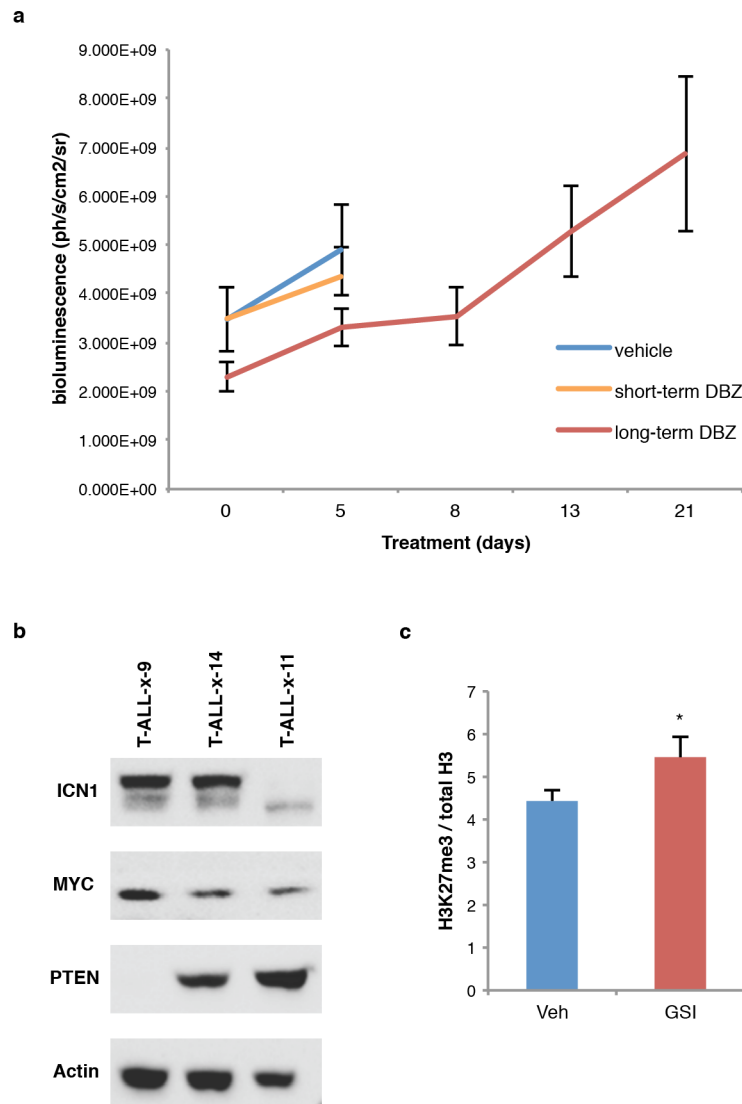


Supplementary Figure 5. BRD4 binds enhancers near key regulatory genes in DND-41 T-ALL cells. **a.** Heatmap shows enrichment signals for BRD4, H3K27ac and H3K4me1 over 19,386 H3K4me1-marked distal sites (rows; 10 kb regions, centered on H3K4me1 peaks, ranked by overall signal intensities of BRD4 and

H3K27ac) in DND-41 persister cells. **b.** Tracks show BRD4 binding and H3K36me3 enrichment (marks transcribed regions) over the *CDK6* and *ETV6* loci, both of which contain BRD4-bound ‘super-enhancers’. **c.** Tracks show BRD4 binding and H3K27ac enrichment across the *DTX1* (left) and *LGALS9* (right) loci in naïve and persister DND-41 cells. **d.** Tracks show BRD4 binding and H3K36me3 enrichment across the *BCL2* locus in naïve and persister DND-41 cells (left). BRD4 enrichment by ChIP-qPCR over BRD4 peaks in the *BCL2* locus in naïve and persister DND-41 cells (right; 2 replicates, error bars reflect s.d.). **e.** Western blots show *BCL2* expression after lentiviral infection with empty vector (EV) or *BCL2* ORF in persister cells. **f.** Tracks show BRD4 binding and H3K36me3 enrichment across the *MYC* locus in naïve and persister DND-41 cells (left). BRD4 enrichment by ChIP-qPCR over BRD4 peaks in the *MYC* locus in naïve and persister DND-41 cells (right; 2 replicates, error bars reflect s.d.). **g.** *MYC* expression in persister cells infected with empty vector (EV) or *MYC*-overexpressing retrovirus (*MYC*; 2 replicates, error bars reflect s.d.). (Data shown for DND-41 cells; data for KOPT-K1 cells in Figure 3.)



Supplementary Figure 6. Proposed model for the increased BRD4 dependency in persister cells. Enhancer elements with transcription factor (TF) binding, acetylated chromatin and BRD4 are flanked by compact chromatin. Tendency of persister cell chromatin (right) towards greater compaction renders enhancers more dependent on BRD4 for their maintenance.



Supplementary Figure 7. Effects of combination therapy targeting NOTCH and BRD4 *in vivo*. **a.** Bioluminescence readings in NSG mice engrafted with KOPT-K1 T-ALL cells expressing luciferase that were treated with vehicle, short-term DBZ (3 doses) or long-term DBZ (with every other day dosing; short-term and vehicle treated mice sacrificed after 5 days (3 doses DBZ), long-term treated mice after 3 weeks (11 doses DBZ); see methods). Data are averaged from 5 mice per group, error bars reflect s.d. **b.** Western blots show intracellular NOTCH1 (ICN1), MYC, PTEN and Actin control in three primary T-ALL samples (T-ALL-x-9, T-ALL-x-11 and T-ALL-x-14). **c.** Bar plot indicates relative levels of H3K27me3 per ELISA on bulk histones from vehicle (Veh) or GSI-treated mice engrafted with T-ALL-x-9 after three week treatment (4 mice per group with 2 replicates each, error bars reflect s.d., * = p value < 0.05).

Supplementary Table Legends:

Supplementary Table 1: Geneset enrichment analysis of persister DND-41 and KOPT-K1 cells compared to naïve DND-41 and KOPT-K1 T-ALL cells.

Supplementary Table 2: Z-scores of hairpins (TRC ID = Name) in naïve (N1 and N2) and persister (P1 and P2) DND-41 cells.

Supplementary Table 3: Genes associated with top-ranked BRD4 peaks in persister DND-41 (sumSignal_DND-41_Persister) and KOPT-K1 (sumSignal_KOPT-K1_Persister) cells.

Supplementary Table 4: Summary of patient characteristics and treatment responses. **a.** Patient characteristics. **b.** Responses to vehicle treatment, single agent DBZ or JQ1 and combination therapy of DBZ and JQ1 for 3 patient samples (T-ALL-x-9, T-ALL-x-11, T-ALL-x-14) engrafted into NSG mice. The table lists days treatment was started and the latency periods for vehicle, single agent DBZ or JQ1 and combination therapy. P values and number of mice treated for the respective samples are listed.

Supplementary Table 5: Gene expression primer sequences, CHIP-PCR primer sequences and shRNA target sequences.

Supplemental Table 4: Summary of patient characteristics and treatment responses.**a. Patient characteristics**

Patient ID	Sample type	Age (years)	Sex	Immuno-phenotype	NOTCH1 expression	PTEN expression
TALL-x-9	Diagnostic	4	F	CD45, CD3, CD4, CD8, CD5, CD2, CD7, TdT	Positive	Negative
TALL-x-11	Relapse ETP	20	M	CD45, CD34, CD7, CD117, CD56	Positive	Positive
TALL-x-14	Relapse	5	M	CD45, CD2, CD3, CD4, CD5, CD7, CD8, CD10	Positive	Positive

b. Treatment responses

Latency Days					
Patient ID	Treatment Start	Vehicle	DBZ	JQ1	DBZ and JQ1
T-ALL-x-9	49 days	86 days (n=5)	120 days (n=5) p = 0.0020 compared to vehicle	113 days (n=5) p = 0.0020 compared to vehicle	153 days (n=4) p = 0.0047 compared to vehicle p = 0.0074 compared to DBZ p = 0.0067 compared to JQ1
T-ALL-x-11	110 days	141.5 days (n=4)	153 days (n=5) p = 0.0564 compared to vehicle	150 days (n=5) p = 0.1715 compared to vehicle	179 days (n=4) p = 0.0067 compared to vehicle p = 0.0040 compared to DBZ p = 0.0038 compared to JQ1
T-ALL-x-14	21 days	54 days (n=5)	80 days (n=5) p = 0.0027 compared to vehicle	66 days (n=5) p = 0.0082 compared to vehicle	84 days (n=4) p = 0.0065 compared to vehicle p = 0.0120 compared to DBZ p = 0.0074 compared to JQ1

Supplementary Table 5: Gene expression primer sequences, ChIP-PCR primer sequences and shRNA target sequences.Gene expression primer sequences

	Forward Primer	Reverse Primer
GAPDH	CTCCTGTTTCGACAGTCAGCC	ACCAAATCCGTTGACTCCGAC
β 2-microglobulin (β 2M)	GAGGCTATCCAGCGTACTCCA	CGGCAGGCATACTCATCTTTT
HP1 γ	TAGATCGACGTGTAGTGAATGGG	TGTCTGTGGCACCAATTATTCTT
HES4	CCTGGAGATGACCGTGAGACA	TACTTGCCCAGAACGGCG
DTX1	TCCCGGTGAAGAACTTGAATG	ACAGCAGTATCCCGGTCAT
BCL2	TTGTTCAAACGGGATTCACA	GGCTGGGCACATTTACTGTT
BRD4	GAATAGTGCCGTGGAGGTGT	ACACAGGTGGGAAGGAACTG

ChIP primer sequences

	Forward Primer	Reverse Primer
MYC	GAGCAGCAGAGAAAGGGAGA	CAGCCGAGCACTCTAGCTCT
BCL2	GCAACGATCCCATCAATCTT	GTCTGGGAATCGATCTGGAA
BC (background control)	CCTAGGCAACAGTGACACCTATTT	AAAAATCAGTTTGTGTGTTTGTGG

shRNA target sequences

Name	TRC ID	Target Sequence
shBRD4-1	TRCN0000199459	5'-GCCTATGTCCTATGAGGAGAA-3'
shBRD4-2	TRCN0000199427	5'-CAGTGACAGTTCGACTGATGA-3'
sh ctrl-1	TRCN0000072182	5'-TCTCGGCATGGACGAGCTGTA-3'
sh ctrl-2	TRCN0000072236	5'-CCAACGTGACCTATCCATTA-3'

Supplementary Note:

Primary human T-ALL samples were obtained from children with T-ALL enrolled in clinical trials of the Dana-Farber Cancer Institute. Samples were collected with informed consent and with approval of the institutional review board. This study was conducted in accordance with the Declaration of Helsinki. Routine immunophenotyping included flow-based analysis for CD3, CD4, CD8, CD5, CD2, CD7, CD45, CD34, CD117, CD56, CD8, CD10 and TdT. Leukemic blasts were isolated from peripheral blood or bone marrow by Ficoll-Hypaque centrifugation and cryopreserved in FBS containing 10% dimethylsulfoxide (DMSO) and stored in liquid nitrogen. Fresh or frozen leukemic blasts were expanded in NSG mice by transplanting 0.5 to 5 x 10⁶ viable leukemic cells via intravenous injection. Primary human T-ALL samples were isolated from the spleen and bone marrow of NSG mice and further processed as described in Methods.